



## Influence of the geometrical parameters in flue instruments on the vorticity modulation near the separation points of the jet

F. Blanc<sup>a</sup>, P.-Y. Lagrée<sup>b</sup>, P. De La Cuadra<sup>c</sup> and B. Fabre<sup>a</sup>

<sup>a</sup>Institut Jean Le Rond d'Alembert / LAM (UPMC / CNRS / Ministère Culture), 11, rue de Lourmel, 75015 Paris, France

<sup>b</sup>Institut Jean le Rond d'Alembert - FCIH team, 4 place Jussieu, 75006 Paris, France

<sup>c</sup>Centro de Investigación en Tecnologías de Audio (CITA), Universidad Católica de Chile, Alameda 340, Oficina 13, Casilla 114-D Santiago, Chile

blanc@lam.jussieu.fr

The geometry of the exit of the channel has a great influence on the behaviour and the tone quality of flue instruments. According to makers, it is a very sensitive point.

Previous works show that variations of the geometry of the exit of the channel has little influence on the velocity profile of the jet and on the position of the separation points. Thus, variations of the geometry are expected to affect mainly the interaction between the air jet and the acoustic field.

The paper will present measurements along with direct Navier Stokes calculations for different geometrical configurations of a jet emerging in a transverse oscillating velocity field. We investigate the modulation of the vorticity of the jet shear layers by the acoustical field, in the vicinity of the separation points, in an attempt to develop a model that allows to predict the influence of the geometry.

## 1 Introduction

In flue instruments, the excitation is created by the oscillation of an air jet around the labium, sustaining the acoustic wave in the resonator. The acoustic wave disturbs the jet in return, ensuring the feedback loop [1].

The receptivity to disturbances of the jet and its velocity profile are thus important parameters. The mouth pressure range for the oscillation and the timbre of the instrument may also depend on them [2].

In the flute, the musician controls the shape of the geometry of the excitator, and adapts it to the playing conditions. In particular, the channel is made by the lips of the player, defining a rounded time dependent geometry.

In the making of the recorder, great care is given to the shape of the chamfers at the exit of the channel. Makers insist on the need of sharp chamfers [2], for a good tone quality. Recorders made with rounded chamfers present a noisy sound. Makers have to compromise with the jet parameters in all the blowing and frequency range.

Previous work on the jet birth involving flow visualisation and numerical simulations [3] showed that the geometry of the exit of the channel has little influence on the velocity profile, the width of the jet, and on separation points.

In this paper, we investigate the influence of different geometries on the behaviour of a jet emerging in an oscillating velocity field. Both jet visualisation and numerical simulations are used.

The studied system is a simplified two-dimensional configuration with neither labium, nor a resonator. The jet emerges from an artificial mouth, whose exit geometry can be changed. Three geometries are used : a squared exit, a 45 degrees chamfered exit, and a rounded exit [3].

An attempt to develop a model of the interaction between the jet and the acoustic perturbation, taking into account the geometry of the exit of the channel is presented.

## 2 Flow visualisation

### 2.1 Experimental configuration

The experimental setup consists on a jet emerging from an artificial mouth and submitted to a sinusoidal acoustic perturbation [4]. In all the geometries, the flue exit is  $1mm$  high and  $20mm$  wide. Such dimensions ensure a two-dimensional behaviour of the jet. The perturbation is provided by two loudspeakers with opposite phases.

A couple of microphones is used to measure the acoustic velocity in the direction perpendicular to the jet plane (Fig.1). The Schlieren method is used to visualise the flow, and image processing is used to detect the jet position [5].

The mouth pressure is measured, and is used to estimate the jet center velocity  $U_0$  with the Bernoulli equation (1).

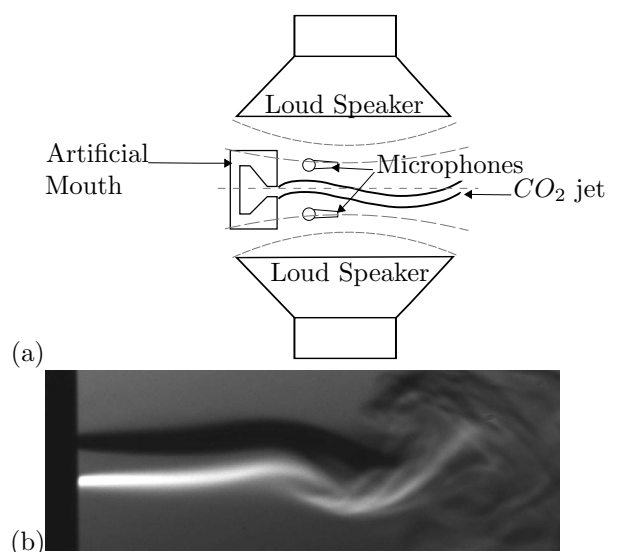


Figure 1: (a) Experimental setup used for the flow visualisations; (b) example of a visualisation with the setup

$$U_0 = \sqrt{\frac{2p_m}{\rho}} \quad (1)$$

We also define the Reynolds number  $Re$  and the Strouhal number  $Str$  as follows :

$$\begin{cases} Re &= \frac{U_0 h}{\nu} \\ Str_h &= \frac{\omega h}{U_0} \end{cases}, \quad (2)$$

where  $\nu$  is the cinematic viscosity of the gas ( $CO_2$ ),  $h$  the channel height and  $\omega$  the pulsation of the loudspeakers. Typical values of  $Re$  are between 100 and 1000, and values of  $Str_h$  are between 0.1 and 1.4. In flue instruments,  $Str_W$  is usually defined with the distance  $W$  between the flue exit and the labium ( $h \leq W \leq 10h$ ).

Different geometrical configurations (rounded or sharp) can be used at the exit of the channel.

### 2.2 Experimental results

The jet is assumed to follow a linear description, leading to a transverse displacement  $\eta$  following Eq (3), where

$c_p$  is the perturbation propagation velocity [6, 7, 4]:

$$\eta(x, t) = \Re\left(\eta_0 e^{\alpha x} e^{-i\omega(t-x/c_p)}\right) \quad (3)$$

Using jet detection algorithms, we can evaluate the parameters  $\eta_0$ ,  $\alpha$  and  $c_p$  of the jet displacement. The parameter  $\eta_0$  is measured by extrapolating the growth of the jet perturbation to the origin of the jet. Thus it is not a physically reliable parameter.

Fig.2 shows the evolution of  $\alpha$  as a function of the Strouhal number [4]. The evolution of this parameter does not seem to be dependent of the geometry of the exit of the channel. It reaches a maximum at  $Str_h \approx 0.5$ .

The ratio  $\frac{\eta_0 U_j}{v_{ac} h}$  is displayed on Fig.3. The dispersion is stronger : although it is hard to extract tendencies, it is clear that the evolution of this ratio depends on the geometry of the flue exit.

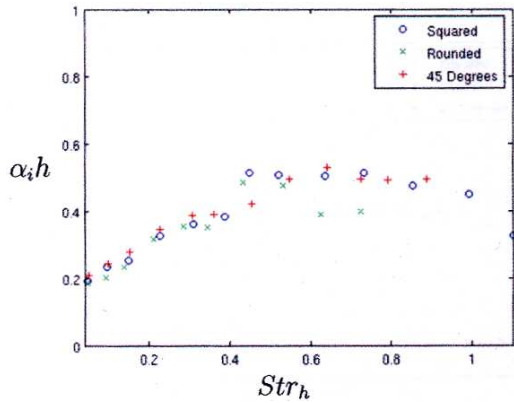


Figure 2: Measurement of  $\alpha h$  as a function of the Strouhal number

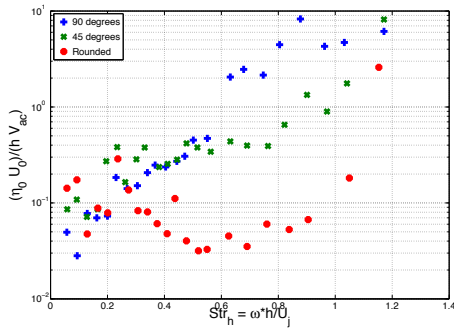


Figure 3: Experimental measurement of  $\frac{\eta_0 U_j}{v_{ac} h}$ . The ratio is of the order of magnitude of the unity

### 3 Numerical simulations

#### 3.1 Simulation description

A two-dimensional incompressible Navier-Stokes solver is used to compute the experimental configuration [3]. The simulation domain is opened with outflow boundary conditions, with imposed  $p = 0$ . Above and under the mouth, in order to simulate the loudspeakers, boundaries are replaced with a no slip condition and an imposed oscillating normal velocity, as shown in Fig.4.

A Poiseuille flow is imposed at the entrance of the channel, and a tracer is injected within the jet. The Strouhal and Reynolds numbers in the simulations are scaled to fit with the experimental data.

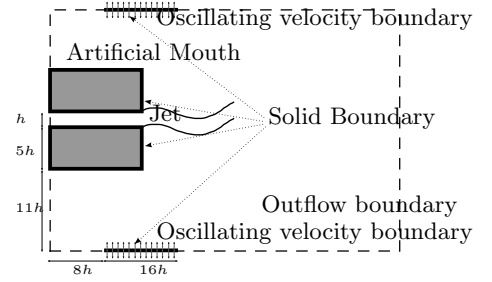


Figure 4: Schematics of the simulation domain

As with experimental data, jet detection is made, so that we can estimate  $\eta_0$ ,  $\alpha$  and  $c_0$ . The jet detection is made using the concentration of the tracer (Fig.5). As the jet detection is made column by column, the detection is only valid before the first roll-up.

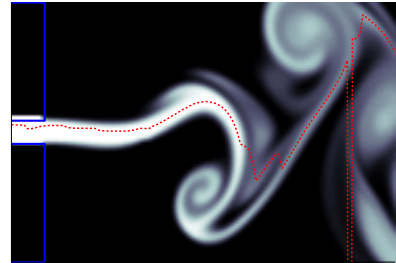


Figure 5: The jet is detected in the simulations, using the concentration of the tracer

The transverse displacement of the jet is then projected on a sine function with the frequency of the excitation for each distance from the mouth. Fig.6 shows the displacement of the jet and the fitted displacement.

The fitted displacement gives us informations on the amplitude and the phase of the oscillation of the jet, from which we can extract the jet parameters (Fig. 7). An exponential fit of the amplitude of the oscillation gives us estimations of  $\eta_0$  and  $\alpha$ .

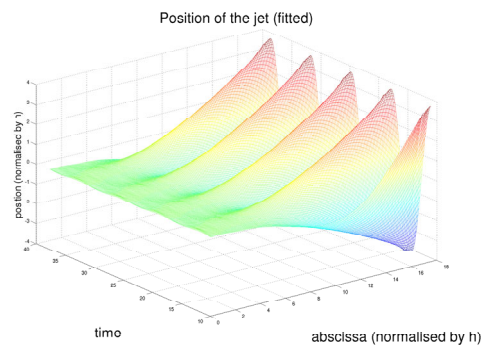


Figure 6: (a) Transverse position of the jet as a function of the distance from the mouth and the time, fitted with an oscillating exponential

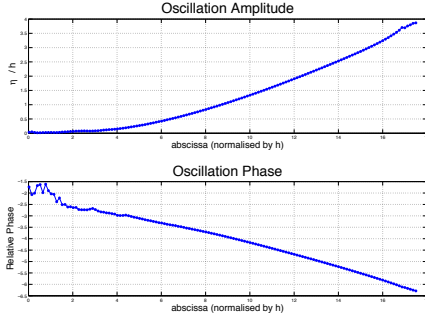


Figure 7: Evolution of the amplitude and the phase of the oscillation of the jet with the distance from the mouth

### 3.2 Simulation results

As for the experimental work, numerical simulations are done for different geometrical configurations and excitation frequencies. Here, the results for three long channels with the different exit geometries are presented.

Considering Fig.8, one can see that in the simulations  $\alpha h$  fits well with the experimental results[4]. For values of  $Str > 0.5$ , jet detection becomes unreliable, and gives erroneous values of  $\alpha h$ .

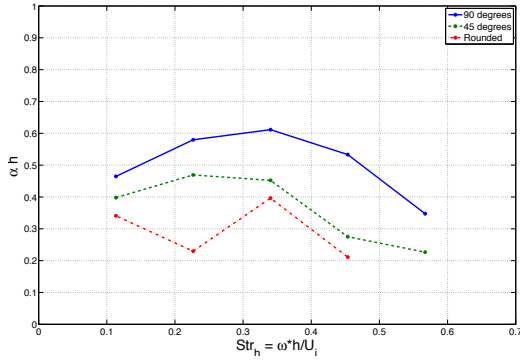


Figure 8: Evolution of the parameter  $\alpha h$  with the Strouhal number for the three simulated configurations

Figure 9 shows the evolution of  $\frac{\eta_0 U_j}{v_{ac} h}$  with the Strouhal number. Although simulations seem to overestimate the experimental results, their results are of the same order of magnitude.

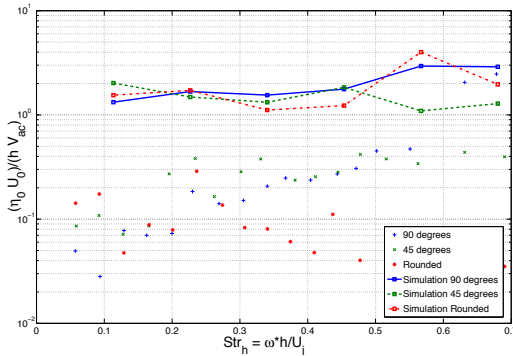


Figure 9: Evolution of the parameter  $\frac{\eta_0 U_j}{v_{ac} h}$  with the Strouhal number for the three simulated configurations

### 3.3 Simulations validation

One key point in the simulations is to measure the velocity field created by the oscillating boundaries. In order to estimate it, simulations have been done, without a jet emerging from the channel. Figure 10 shows the amplitude of the perturbation field in front of the flue exit. The velocity is not homogeneous : a boundary layer develops near the mouth. As the acoustical field is simulated by a boundary condition for the velocity, it is interesting to compare this boundary layer with the theoretical acoustic boundary layer.

In the simulation presented on figure 10,  $Re = 200$ , and  $Str_h = 0.2$ , which corresponds to a frequency of  $f = 100Hz$ , and a jet central velocity of  $U_0 = 3ms^{-1}$ . The acoustical boundary layer is given as follows :

$$\delta_v = \sqrt{\frac{2\nu}{2\pi f}} \quad (4)$$

This gives in this particular case a thickness of  $0.2mm = 0.2h$ . On Fig.10 are also represented the theoretical boundary layer, and the first order developpement of it. The boundary layer seems to be a bit under-estimated, but the orders of magnitude are comparable.

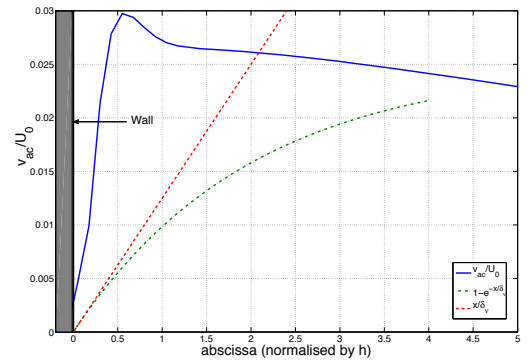


Figure 10: Amplitude of the perturbation field in front of the flue exit ( $Re = 200$  and  $Str_h = 0.2$ )

## 4 Developing a model of the interaction

### 4.1 Basis of the model

Looking at the velocity field of the excitation near the flue in the simulation, the perturbation of the jet appears to be a consequence of the velocity of the perturbation penetrating in the channel.

Here, we model the interaction in the simplest way. We only consider a parallel flow ( $U_0(y)$ ) in a channel with an oscillating perturbing velocity field. Depending on the geometry at the flue exit, the perturbing flow may be decomposed in two contributions : one in the flow direction ( $u_w$ ), and one normal to the flow direction ( $v_w$ ). The perturbation results in a correction ( $\tilde{u}$ ) in the velocity field (Eq(5)) : the perturbed flow remains parallel.

$$\begin{cases} u &= U_0(y) + (\tilde{u}(x, y) + u_w)e^{i\omega t} \\ v &= 0 + v_w e^{i\omega t} \end{cases} \quad (5)$$

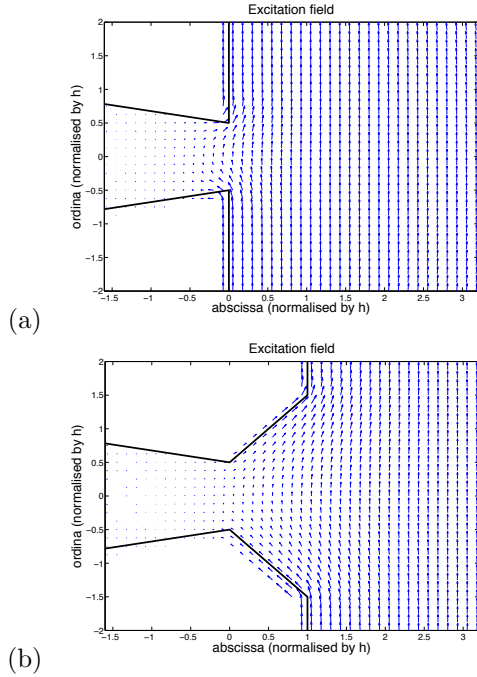


Figure 11: Velocity field created near the flue by the oscillating velocity boundary conditions (a) with a squared exit, (b) with a chamfered exit. The excitation field penetrate differently in the channel, depending on the mouth geometry

The flow is described as incompressible, and the perturbations are small. We only consider the first order of perturbations.

## 4.2 Resolution

To solve the equations of the model, we need to make further assumptions about the non perturbed flow and the perturbation velocities.

Figure 12 shows the amplitude of the perturbing flow (in the  $x$  and  $y$  directions). As suggested by the simulations, we assume  $v_w$  to be constant and  $u_w$  to grow linearly through the height of the channel. We also assume  $U_0(y)$  to be a Poiseuille flow.

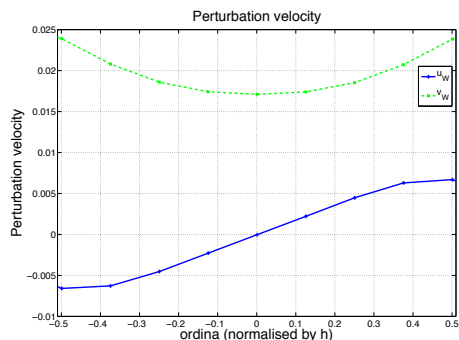


Figure 12: Amplitude of the simulated perturbing flow through the height of the channel, with a squared exit

The equations describing the system then become :

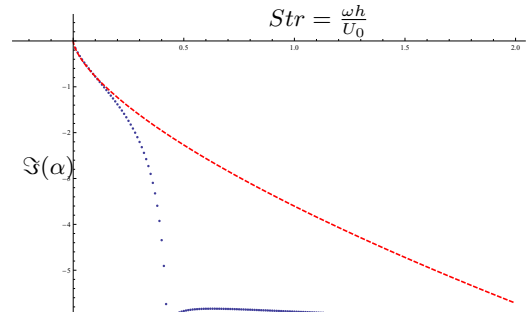


Figure 13: Imaginary part of  $\alpha$  as a function of  $Str$ , given by a numerical resolution of the Rayleigh equation with a Poiseuille flow (dots), the solution for a top-hat jet is also represented (dashed line)

$$\begin{cases} \frac{\partial^2 \tilde{u}}{\partial y^2} - i\omega \tilde{u} &= -2 \frac{y}{\nu h} (v_{w0} \frac{U_0}{h} + i\omega u_{w0}) \\ \tilde{u}(\pm \frac{h}{2}) &= 0 \end{cases} \quad (6)$$

We finally obtain a second order inhomogeneous linear differential equation with boundary conditions, that can be analytically solved.

This model of the interaction leads to a distorted Poiseuille flow, which can be linked to a instable jet model.

## 4.3 A model of an instable jet

To ensure continuity with the perturbed flow, the base flow of the jet is described as an invicid Poiseuille flow. Rayleigh's theory of linear instability is used [6] in order to find the perturbing stream function :

$$\psi(x, y, t) = \Re \left( \phi(y) e^{i(\alpha x - \omega t)} \right) \quad (7)$$

The dispersion relation is computed numerically. The imaginary part of  $\alpha$ , which corresponds to the growth of instability is represented in Fig.(13). The dispersion relation of a top-hat profile is also represented [8]. The instable Poiseuille flow is expected to be realistic at low value of  $Str$  : it is in good agreement with the top-hat profile for low  $Str$  values.

## 5 Conclusion and future work

In this paper, experimental work is simulated using a two-dimensionnal Navier-Stokes solver. Results of the simulations are in good agreement with experimentations.

A very simple model of the interaction between the jet and the acoustical field is also presented. This model is inspired by observations on the simulations.

Simulations provide parameters to feed the model, and agreement between both can be verified. Hot wire measurement of the velocity profile of the flow at the exit of the channel can also be used to validate both simulation and model.

The model of the interaction should also be linked to a model of the resulting jet.

## Acknowledgements

The authors wish to thank Stéphane Popinet for his work on developing the gerris flow solver. Gerris homepage is <http://gfs.sourceforge.net>

## References

- [1] L. CREMER and H. ISING. Die selbsterregten schwingungen von orgelpfeifen. *Acustica*, 19(3):143–153, 1967-1968.
- [2] C. SÉGOUFIN. *Production de son par interaction écoulement/résonateur acoustique : Influence du système amont, application à la flûte à bec*. PhD thesis, Université Pierre et Marie Curie, 2000.
- [3] F. BLANC, P.-Y. LAGRÉE, B. FABRE, and A. ALMEIDA. Influence of the geometry of the channel exit on the jet birth in flue instruments. In *Proceedings of Isma 2007*, 2007.
- [4] P. de la CUADRA. *The sound of oscillating air jets : Physics, modeling and simulation in flute-like instruments*. PhD thesis, University of Stanford, 2005.
- [5] P. de la CUADRA, C. VERGEZ, and B. FABRE. Visualization and analysis of jet oscillation under transverse acoustic perturbation. *Journal of Flow Visualization and Image Processing*, 14:355–374, 2007.
- [6] J. W. S. RAYLEIGH. *The Theory of Sound*. Dover, New York, 1877.
- [7] G. E. MATTINGLY and W. O. CRIMINALE. Disturbance characteristics in a plane jet. *The physics of fluids*, 14:2258–2264, 1972.
- [8] M.-P. VERGE. *Aeroacoustics of confined jets with applications to the physical modeling of recorder-like instruments*. PhD thesis, Technische Universiteit Eindhoven, 1995.